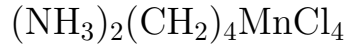


Chaotic regimes of antiferromagnetic resonance in a quasi-two-dimensional easy-axis antiferromagnet



M. M. Bogdan, M. I. Kobets, and E. N. Khats'ko

*B. Verkin Institute for Low Temperature Physics and Engineering,
National Academy of Sciences of the Ukraine, 310164 Kharkov, Ukraine*

E-mail: bogdan@ilt.kharkov.ua

(Submitted October 23, 1998)

Abstract

Chaotic regimes of the microwave energy absorption are experimentally observed and analyzed for two-dimensional metallorganic antiferromagnet $(\text{NH}_3)_2(\text{CH}_2)_4\text{MnCl}_4$ at low temperatures under the conditions of nonlinear antiferromagnetic resonance. Relaxation oscillations of energy absorption are investigated in detail. Their frequency spectra, frequency–amplitude characteristics, and dependences of absorbed power on driving power and static magnetic field are studied. It is shown that the dynamics of relaxation oscillations undergoes a transition to chaos by “irregular periods”. Peculiarities of the transition are described consistently. Among other things, the conditions for the emergence of energy absorption regimes with a spike-like and a saw-tooth signal structure are determined, and the characteristics of chaotic oscillations such as the dimensions of strange attractors are calculated. The chaotic dynamics is found to be high-dimensional with a large contribution from noise which is of deterministic origin in the antiferromagnet under in-

vestigation.

Fiz. Nizk. Temp. **25**, 263–276 (March 1999)

INTRODUCTION

Chaotic resonant phenomena in magnets have become an object of intense experimental studies in the last decade.^{1–19} These investigations were stimulated by the progress made in the mathematical theory of chaos predicting the universal character of chaotic phenomena irrespective of the nature of the physical object being studied and demonstrating a nonlinear behavior.^{20–22}

Magnetic compounds possessing the properties required for the emergence of nonlinear oscillations include first of all the crystals exhibiting an extremely weak relaxation of spin excitations. Yttrium–iron garnet (YIG) with a low threshold for a parametric excitation of spin waves even at room temperature has been studied most thoroughly.^{1,5,8,9,11–13} Since YIG behaves as a ferromagnet in the magnetic respect, nonlinear chaotic effects were studied, as a rule, under the conditions of ferromagnetic resonance (FMR) in a transverse as well as longitudinal driving fields.

The total number of investigated nonlinear magnet is not large, and some of them exhibit nonlinear properties only at low temperatures of the order of a few kelvins, at which phonons are frozen out, and their interactions with magnons becomes very weak.

The effective dimensionality of crystals plays an important role for the suppression of relaxation processes. Stepanov et al.^{14–18} investigated the class of metallorganic compounds that are quasi-two-dimensional ferro- and antiferromagnets in the magnetic respect. It was found that low-dimensional magnets at low temperatures go over to a state with an anomalously low spin–lattice relaxation virtually with a threshold, which makes it possible to excite spin waves parametrically at microwave pumping power of the order of a few milliwatts.¹⁸ Among other things, it was found that in addition to YIG, nonlinear ferromagnetic crystals include metallorganic compounds with a structure similar to the $(\text{CH}_3\text{NH}_3)_2\text{CuCl}_4$ crystal.¹⁹ On the other hand, it was established that chaotic oscillations are generated in the crystals $\text{CuCl}_2\cdot 2\text{H}_2\text{O}$,² CsMnF_3 ,^{6,10} $(\text{CH}_2\text{NH}_3)_2\text{CuCl}_4$ ⁹ under the conditions of antiferromagnetic resonance (AFMR).

The range of nonlinear effects that have been discovered and thoroughly investigated in ferro- and antiferromagnets is quite large. These include spin-wave instabilities (Suhl instabilities of the first- and second order),²³ auto-oscillations of absorbed microwave power,^{24,25} and the observation of three known scenarios of a transition to chaos: by period doubling (Feigenbaum scenario), quasiperiodicity, and intermittency.^{20–22}

Apart from the interpretation of these nonlinear effects and the determination of the conditions for their observation, it was found that real magnetic crystals can demonstrate a more complex pattern of transition to chaotic regimes in resonance experiments. None of the known scenarios is realized in pure form in such cases,²⁶ and we must consider new mechanisms of chaotization.^{3,5,27}

Hartwik et al.²⁸ were the first to discover long ago the so-called relaxation chaotic oscillations of microwave power in YIG with which a new scenario of a transition to chaos by irregular periods has been associated in last decade.^{3,8,9,29} This effect lies in the emergence, instead of purely periodic auto-oscillations, of irregular chaotic bursts of absorbed power in the form of spike-like peaks or pulses with a steep leading front and relaxing rear front under certain conditions of magnetic resonance upon an increase in the pumping power. Theoretical approaches to the description of such oscillations and mechanisms of their formation were made in Refs. 9,29,30, but a systematic analysis of temporal series of experimental signals as well as of the results of numerical simulation of relaxation oscillations was carried out only recently.^{31,32}

In this work, we study experimentally the regimes of chaotic behavior of the microwave power absorbed in a two-dimensional easy-axis antiferromagnet $(\text{NH}_3)_2(\text{CH}_2)_4\text{MnCl}_4$ under the AFMR conditions. This compound is a typical representative of the family of layered Heisenberg antiferromagnets $[\text{NH}_3-(\text{CH}_2)_m-\text{NH}_3]\text{MnCl}_4$ (2CmMn) studied by Stepanov et al.^{14–18} The structure of these metallorganic crystals is formed by almost quadratic layers of magnetic ions in the octahedral environment of chlorine ions between which long chains of alkylene–ammonia molecules are located. The small value of interlayer exchange associated with a large separation between the spins of adjacent layers leads to a quasi-two-dimensional

behavior of these systems. At temperature $T_N = 42.6$ K,³³ the compound 2C4Mn is transformed into the antiferromagnetic states with the easy magnetization axis directed at right angles to the planes of the layers. A detailed analysis of linear antiferromagnetic resonance in 2C4Mn revealed¹⁶ that this compound has a four-sublattice noncollinear antiferromagnetic structure with a weak ferromagnetic moment. The antiferromagnetism vector of each layer is deflected successively from the normal to the plane of a layer through an angle of $\pm 16^\circ$ so that the total vector is perpendicular to the layer, and the weak antiferromagnetism vector lies in the layer. According to estimates, the strength of interaction between the layers (26 Oe) is extremely small as compared to both the intralayer exchange ($2H_e \simeq 1360$ kOe) and the intralayer uniaxial anisotropy ($H_a \simeq 0.8$ kOe) so that 2C4Mn can be regarded as an almost two-dimensional antiferromagnet.

At low temperatures (of the order of a few kelvins), the related compound $(\text{NH}_3\text{C}_2\text{H}_5)_2\text{MnCl}_4$ (1C2Mn) revealed a number of interesting nonlinear phenomena in the behavior of the absorbed microwave power, e.g., the emergence of auto-oscillations and chaos.¹⁸ Here we carry out a systematic analysis of chaotic regimes of antiferromagnetic resonance in a 2C4Mn crystal. For a driving power below 5 mW at a temperature below 2.18 K, we observed a nonlinear absorption of the microwave field and the emergence of relaxation oscillations with typical (extremely low) average frequencies of the order of a few hertz. These oscillations were recorded and analyzed as temporal series of data with the help of an analog-digital device and computer programs, which made it possible to describe in detail description of the scenario of a transition to chaos by irregular periods. As a result, we have analyzed qualitative changes in the behavior of temporal series of absorbed power as a function of variation of the parameters of static and varying magnetic fields and carried out the Fourier analysis, obtained the spectra of oscillations, studied the structure of strange attractors of chaotic regimes, and calculated the quantities characterizing chaotic dynamics, i.e., dependences of frequencies of auto-oscillations oscillations on the driving power (in particular, we determined their period doubling threshold) and the dimension of chaotic attractors, and discussed the origin and role of noise in relaxation oscillations as

well as a possible theoretical model for describing relaxation oscillations in two-dimensional antiferromagnets.

EXPERIMENTAL TECHNIQUE

Single crystals of $(\text{NH}_3)_2(\text{CH}_2)_4\text{MnCl}_4$ were grown at room temperature from a saturated aqueous solution in the form of thin rectangular plates with clearly manifested lateral faces and with a typical size $5 \times 5 \times 0.3$ mm. The compound $(\text{NH}_3)_2(\text{CH}_2)_4\text{MnCl}_4$ possesses a monoclinic symmetry of crystal lattice with the space group $P2_1/b$.³⁴ Organic chains of $\text{NH}_3(\text{CH}_2)_4\text{NH}_3$ separate two-dimensional almost square layers of octahedra Mn-Cl_6 . The unit cell parameters are $a = 10.77$ Å, $b = 7.177$ Å, $c = 7.307$ Å. Experiments were carried out on a reflection spectrometer with a pumping frequency 70.39 GHz at a temperature below 2.18 K. We used a cylindrical resonator with the Q -factor ~ 1000 . The sample was placed in the resonator region with predominant parallel polarization of external static and rf fields $H \parallel h$.

In resonance experiments, the field is usually applied along the easy axis of the crystal. With such an orientation, the splitting of AFMR branches follows the law

$$\omega_{\pm} = \gamma \left\{ \sqrt{(2H_E + H_A)H_A} \pm H \right\} \quad (1)$$

For the frequency mentioned above, the resonance conditions are satisfied for the lower frequency branch ω_- , which was observed in our experiments. The maximum power of the source was 5 mW. The applied magnetic field was scanned along the contour of the AFMR line, and the driving power was varied from 0 to -20 dB. The magnetic field orientation relative to the anisotropy axis and equilibrium directions of antiferromagnetism vectors in adjacent planes also varied. It was found that the most intense absorption corresponds to the symmetric orientation of the field along the crystallographic axis b .

In all experiments, low-frequency modulation of electromagnetic field of frequency 50 Hz was observed. This frequency had to play the role of the reference frequency in our experiments. It was found later that these oscillations participated in all nonlinear processes, and

the emergence of their higher harmonics was regarded as a natural criterion of the emergence of nonlinearity in resonance effects. The reflected signal after detection in an analog-digital device PC ADDA-14 with a 14-bit resolution was transformed into a computer data file. These temporal series were subsequently analyzed by using the standard and original packets of programs created for a quantitative analysis of chaotic phenomena.

DISCUSSION OF MAIN RESULTS

A typical form of resonant curves for the antiferromagnet 2C4Mn at $T = 1.8\text{ K}$ are shown in Fig. 1. For a low (less than -15 dB) microwave field power, a typical pattern from a linear AFMR is observed, i.e., two lines from two centers (neighboring planes). The separation between the peaks on the resonant curve can vary depending on the orientation of the static magnetic field, and the lines can coincide when the field is directed along the crystallographic axis b . For a power exceeding -15 dB , free relaxation oscillations are generated in the range of external magnetic fields near the peak of the high-field line above as well as below the resonant field $H = 9.34\text{ kOe}$ (this region is shown by the bold line on the upper curve in Fig. 1). The amplitude of these oscillations increases with power until they become chaotic. We shall consider this regime in detail later, and now we pay attention to another effect associated with instability of resonance at high pumping levels. As the driving power increase above -5 dB (see two lower curves in Fig. 1), a jump and a discontinuity of both resonant lines are observed with a considerable hysteresis in the static magnetic field as we move towards higher and lower fields respectively.

This phenomenon is well known in the theory of nonlinear resonance and is associated with the dependence of the frequency of nonlinear oscillations on their amplitude. In magnets, this effect is manifested in that the resonant curve must become asymmetric and multiple-valued for a pumping field h exceeding the critical value, i.e., the peak must be inclined towards lower or higher fields depending on the type of interaction between magnons. In actual experiments, instability is observed upon a change in the static magnetic field, and

the resonant curve experiences a discontinuity or a jump. This effect was observed for the first time in disks of yttrium-iron garnet single crystals by Weiss.³⁵

It follows from Fig. 1 that the jump is observed in strong fields in an increasing field, while discontinuity takes place in weaker fields in a decreasing field. With increasing power, the hysteresis loop increases, and the steepness of lines decreases (the scales of conditional units for absorbed power in Fig. 1 are different for the three resonant curves: it decreases with increasing amplitude of pumping).

It was noted above that oscillations of observed power on the segment of the resonant curve near 9.34 kOe appear even at very low driving powers of the order of -15 dB. The criterion of a transition to the nonlinear regime is the emergence of the second harmonic peak in reference oscillations with frequency 100 Hz. At the point of maximum on the resonant curve, this peak exceeds the background noise for a power $P > -15$ dB, and first spike-like peaks of absorbed power appear at the same instant.

In the case of a resonant curve with spaced peaks, an increase in the driving power induces relaxation oscillations in the vicinity of the second peak also. As the peaks converge, the mutual effect of the centers increases, which is noticeably reflected in the form of oscillations of absorbed power. In the cases of closely spaced peaks for the value of the field $H_m = 8.37$ kOe corresponding to a local minimum at the center of the resonant curve, relaxation oscillations become irregular even for a low driving power. As the power increases, the oscillations become more and more chaotic. The time dependence of the signal typical of the entire series of these measurements and its spectrum for the maximum value of power are shown in Fig. 2*a*.

In order to find out whether such a dependence is a consequence of additive or dynamic noise, stochastic process, or is due to a determinate chaos, we varied in the experiments the orientation of magnetic field and its magnitude. The variations affected strongly the type of oscillations.

It was found that oscillations become less chaotic for the minimum deviation of the magnitude of magnetic field from the extremal value H_m . By way of an example, Fig. 2*b*

shows the time behavior and spectrum of oscillations for $H = 8.4$ kOe and the maximum driving power.

It also turned out that the degree of chaotization of a signal decreases considerably, and its shape changes qualitatively when the magnetic field is directed along the crystallographic axis b , when the resonant lines from two centers coincide. In this case, the characteristic pattern of the emergence and transformation of relaxation oscillations upon a change in the driving power is of the form shown in Fig. 3 for $H = 8.4$ kOe (small deviation of the field from the resonant value) and the power P varying from -10 to 0 dB. First spikes of absorbed power appear against the background of almost linear oscillations of frequency 50 Hz. For small pumping amplitudes, the frequency corresponding to the emergence of spike-like peaks is low, and the intervals between them are quite large and vary with an obvious periodicity. For a driving power of the order of -6 dB, the signal has the form of a periodic structure of spike-like closely spaced peaks. As the pumping amplitude increases further to power values of the order of -3 dB, the frequency corresponding to the emergence of spike-like peaks changes insignificantly, and subsequently decreases rapidly and becomes virtually equal to half the previous value. In this region, the shape of the signal changes qualitatively from the spike-like to the saw-tooth, i.e., the change in the regime of chaotic oscillations takes place. Figure 4 shows the dependence of the fundamental frequency of these oscillations on the driving power in the range from -6 to 0 dB (solid circles). The doubling of the period of relaxation oscillations can be seen clearly in the figure. In order to plot this dependence, we analyzed the spectra of oscillations for fixed pumping levels. It should be noted that doubling of this period does not indicate the emergence of subharmonics of the fundamental frequency as is usually the case in the Feigenbaum scenario, and corresponds to the change from one oscillatory mode to another mode, their fundamental frequencies differing by a factor of two. It was proved that this effect is preserved for other values of magnetic field which naturally affects the values of frequencies themselves. It should also be noted that apart from the main peaks and multiple harmonics, all spectra contain a large contribution from noise responsible for the “grass-like” continuous spectrum. In the subsequent analysis,

we shall analyze in detail the dynamic and spectral structure of these oscillations and the origin of their stochastic form.

When the power changes in the opposite direction, i.e., the amplitude of pumping decreases (open circles in Fig. 4), the frequency–amplitude dependence exhibits a hysteresis with a displacement of the region of period doubling towards lower powers (saw-tooth pulses exist up to -4.5 dB). The existence of essentially chaotic modes near a certain fixed values of power, in particular upon an increase in the driving power for $P = -1, -2.25,$ and -2.75 dB is an interesting feature of the observed transient process.

For this reason, it was natural to analyze oscillations for these selected pumping levels, but in a wide range of applied magnetic field near the resonance point. We chose the pumping level of -1 dB and studied the variation of the shape of the absorbed power signal and its spectrum upon a change in the static magnetic field within a few ten oersted near the resonant value $H_r = 8.37$ kOe. The direction of the field was maintained along the crystallographic axis b .

The corresponding results are presented in Fig. 5. It should be noted that relaxation oscillations occur against the background of a considerable average absorbed power that must make a contribution to the frequency spectrum in the form of a large central peak at zero frequency. In all calculations of the spectra analyzed here, this average value was subtracted, and hence the given huge contribution to the central peak is absent, which allows us to see the detailed structure of relaxation oscillations proper. It should also be noted that frequency spectra are given in the form of frequency dependences of the amplitude of the Fourier transform of the signal and not as logarithmic spectra of power in order to improve detailization.

Another feature in common of all the spectra considered below is the presence of oscillations of frequency $\nu_0 = 50$ Hz. These low-frequency oscillations were present as a source of reference frequency, but they became involved in free oscillations in view of the nonlinearity of the medium. This follows from the presence of second harmonic with frequency $\nu = 100$ Hz and the peaks that are algebraic sums of frequencies of fundamental harmonics

of relaxation oscillations and the reference frequency.

Far away from the resonant field, the absorbed power is virtually constant if we disregard extremely low background noise in which, however, oscillations with frequency $\nu_0 = 50$ Hz were always manifested (in the frequency spectrum) in our measurements. As the field approaches the resonant level, these small-amplitude oscillations become weakly nonlinear (second harmonic appears in the spectrum), and nearly periodic spike-like peaks of absorbed power corresponding to peaks of the order of a few hertz in the frequency spectrum and clearly distinguishable against the “grass-like” background noise appear almost simultaneously.

A typical example of such a behavior of absorbed power is shown in Fig. 5a for the field value $H = 8.51$ kOe. It can be seen that periodic relaxation oscillations with a spike-like structure have been formed completely. Small anharmonic modulation of peak amplitudes is manifested in the frequency spectrum in the form of higher harmonics of the fundamental frequency. All the remaining peaks can be identified as algebraic sums of these harmonics and frequencies ν_0 and $2\nu_0$.

As we approach the resonant field further, the shape of absorbed power peaks experiences rapid qualitative changes. Figure 5b shows the result of transformation of spike-like signals into typical saw-tooth temporal series for $H = 8.47$ kOe. In addition to the increase in the amplitude and relative height of frequency peaks, the emergence of linearly increasing and decreasing segments on the time dependence of absorbed power is also worth noting. It is remarkable that such oscillations are almost indistinguishable from classical relaxation oscillations that are frequently encountered in electrical engineering.

A subsequent decrease in the field leads to the tendency to the formation of periodic rectangular pulses of absorbed power. Signals of such a shape are shown in Fig. 5c for $H = 8.44$ kOe. It should be noted that the amplitude of oscillations does not increase any longer, while the periodicity is enhanced, which is manifested in the frequency spectrum.

Relaxation oscillations become completely chaotic for field values close to resonance. Figure 5d shows the corresponding temporal series of absorbed power and a typical “grass-like”

frequency spectrum for $H = 8.39$ kOe. It can be seen that the amplitudes of oscillations are much smaller than those in Fig. 5c, and the frequency distribution of oscillations has become almost continuous with a sharp decrease in the maximum peak heights to the amplitude of the 50-Hz peak of the fundamental harmonic.

As the field decreases further from the resonant value, relaxation oscillations again acquire the spike-like shape, being essentially nonlinear. Figure 5e shows for $H = 8.34$ kOe the temporal series for such anharmonic oscillations of absorbed power and their frequency spectrum with clearly manifested peaks of multiple harmonics. A distinguishing feature of these oscillations is that their fundamental frequency is almost half the frequency of similar spike-like oscillations presented in Fig. 5a. The frequency of relaxation oscillations in general decreases as the field decreases to the resonant value, and starts increasing after the passage of the resonance peak.

In the magnetic field scanning in the opposite direction (i.e., upon its increase), the regimes described above appear in the reverse order, but a hysteresis loop takes place in complete accord with the picture shown in Fig. 1.

It was mentioned above that the selection of other values of power (for example, the maximum power $P = 0$ dB) followed by scanning in the static magnetic field results in chaotic nonlinear oscillations whose frequency structure contains higher harmonics of the fundamental frequency as well as subharmonics against the background of a high-intensity continuous noise spectrum (see Figs. 2a and b).

A comparison of temporal series also leads to the conclusion concerning clearly manifested temperature dependence of the degree of stochastization of oscillations. The higher the temperature, the higher the noise level in the oscillatory spectra and the extent of their nonregularity, and vice versa. At low temperatures, we could observe relaxation oscillations in the form of nearly rectangular pulses (such a mode was realized for $P = 5$ mW, $H = 8.3$ kOe, and $T = 1.7$ K).

Another interesting feature is the observation of the regime of an abrupt and virtually complete disappearance of free oscillations with simultaneous doubling of the period of

nonlinear reference oscillations and the emergence of their subharmonic at the frequency 25 Hz. We can try to explain the latter effect from the point of view of the theory of chaos control and the emergence of higher (multiple) resonances. However, we shall not consider this problem here and analyze the structure of chaotic attractors of relaxation oscillations.

ANALYSIS OF EXPERIMENTAL RESULTS

The method of a nonlinear analysis of experimental temporal series has been worked out intensely during the last decade and is described in detail in a number of reviews and monographs.^{19,36–38} We shall use this method which involves the determination of the linear autocorrelation function for temporal series, the determination of “time delay”, the construction of phase portraits of attractors in the corresponding “time delay” coordinates, the construction of interspike intervals and their analysis, the computation of the correlation dimension of attractors, the determination of the noise contribution to temporal series, the source of the noise and possibilities of its reduction and the discussion of theoretical models of the observed chaotic oscillations.

The temporal series is a discrete set of values of the physical quantity (the absorbed power $V(t_n)$ in our case), measured in equal intervals of time. A traditional characteristic of temporal series of signals is the linear autocorrelation function³⁷

$$C_L(\tau) = \frac{\frac{1}{N} \sum_{m=1}^N [s(m+\tau) - \bar{s}][s(m) - \bar{s}]}{\frac{1}{N} \sum_{m=1}^N [s(m) - \bar{s}]^2}, \quad (2)$$

where the average value of the signal $s(m)$ is defined in the standard manner: $\bar{s} = \frac{1}{N} \sum_{m=1}^N s(m)$.

Since we usually subtract the average value of series from the initial series in an analysis of spectra, we calculated autocorrelation function for time dependences presented in Fig. 3 for modified series $\bar{s} = 0$. As a function of τ , it exhibits qualitatively identical behavior for all values of power: this is an oscillating function with a slowly decreasing amplitude. The period of these oscillations coincides with the fundamental period of oscillations of the

signal being measured. In an analysis of nonlinear signals, autocorrelation function is also useful for estimating “time delay”. It is chosen^{19,37} equal to the value of τ for which the autocorrelation function vanishes for the first time. In our measurements, this time delay is approximately equal to a quarter of the fundamental period of observed oscillations.

Figure 6 shows the dependence of time τ on the driving power P . (The unit of measurements of τ is the principal interval $\Delta t = 4.9$ ms of our temporal series.) It can be seen that this dependence obviously correlates with the dependence of the frequency of oscillations on the driving power presented in Fig. 4 and confirms the existence of a threshold transition from one regime of chaotic oscillations to another. It should be noted that the period of the correlation function corresponds to oscillations of frequency 50 Hz for low powers and to the fundamental period of saw-tooth oscillations for the maximum power.

The obtained value of τ can now be used for plotting phase portraits of nonlinear oscillations. For this purpose, we shift the temporal series by τ and plot the dependence of $V(t_n + \tau)$ on $V(t_n)$. These functions are just the time-delay coordinates. For the temporal series corresponding to the maximum power in Fig. 3, the phase portrait is shown in Fig. 7a (the value of τ is chosen equal to 49 ms, and the average value of absorbed power is subtracted from the given series). It can be seen that the process is periodic on the whole and occurs in several stages with their own characteristic times. In order to obtain a more detailed concept of the attractor structure, we constructed a $1D$ map from the sequence of minimum values of the Poincarè sections of the given attractor. These values were determined as negative values of $V(t_m + \tau)$ taken at instants t_m for which $V(t_m) = 0$. This dependence is shown in Fig. 7b and demonstrates the existence of the internal structure of the attractor and an obviously large contribution of noise.

A detailed analysis of the time dependence $V(t)$ indicates that the noise contribution is not additive. Indeed, irregular amplitude jumps as well as periodic oscillations of frequency 50 Hz have different values at different stages of variation of the function $V(t)$. This indicates a nonlinear enhancement of both factors and their participation in the chaotic process.

In order to describe the chaotic behavior of relaxation oscillations and the effect of noise

on them quantitatively, we consider a sequence of time intervals between adjacent peaks of the signal and the sequence of maximum values of peak amplitudes as characteristics of this process.

These dependences of amplitude peaks and interspike intervals for the series under investigation are compared with the relevant sequences for the series shown in Fig. 5a. It can be seen that the amplitude peaks of oscillations of the absorbed power (Figs. 8a and b) behave quite chaotically in the vicinity of a resonance and far away from it. At the same time, the interspike intervals (Figs. 8c and d) exhibit a clearly manifested tendency to a quasiperiodic mode far away from the resonance (Fig. 8d), but random forces acting on the system result in the stochastization of oscillations, which is accompanied by chaotic jumps in the period of oscillations between its four principal values.

We can try to determine whether a noise is stochastic or dynamic by calculating the correlation dimension D of the attractor under investigation. This quantity is defined through the pair correlation integral:

$$C_m(r) = \frac{2}{N(N-1)} \sum_{i \neq j}^N \theta(r - |\vec{y}_m(j) - \vec{y}_m(i)|), \quad (3)$$

where N is the number of measurements, r the correlation radius, $\vec{y}_m(i)$ the vector of dimensions m in the embedding space, whose coordinates are $\{V(t_i), V(t_i + \tau), \dots, V(t_i + (m-1)\tau)\}$, and $\theta(r)$ is the theta function. This function in fact determines the number of pairs of vectors in the m -dimensional space, the separation between which is smaller than the preset distance r . While determining the distance, we presume that the cells into which the phase space is divided have the cubic shape.³⁹ The dimension D is the limit of the expression

$$D = \lim_{m \rightarrow \infty} \frac{d \ln C_m(r)}{\ln(r)} \quad (4)$$

and is usually calculated on the interval r in which the values of the correlation function are not very small.

The sequence of calculated correlation sums for the initial temporal series corresponding to the maximum power in Fig. 3 is presented in Fig. 9 on logarithmic scale (the curves

correspond to the variation of m from 1 to 9 from top to bottom). Numerical differentiation reveals a flat segment according to which the dimension of a strange attractor can be estimated. It was found that it is slightly larger than two (2.25 ± 0.1), but the strong effect of dynamic noise following from the characteristic increase in the steepness of the curves for $\ln(r) < 2.5$ does not allow us to establish the existence of exact limit. We are inclined to interpret the latter quantity as the dimension of a regular attractor. On the other hand, the slope of the curves in the region $1 < \ln(r) < 2.5$ also demonstrates the tendency to a limit that can be estimated as 4.9 ± 0.1 . Such a limiting value can be regarded as the total dimension of the attractor, containing the contribution from a regular attractor and a deterministic noise. A slight increase in the dimension for large values of m for small r is associated with the contribution of “white” instrumental noise. The above comparative analysis of functional dependences of temporal series and their spectra also confirms this conclusion. Thus, the analysis of the correlation dimension leads to the conclusion concerning the dynamic nature of noise in the relaxation oscillations under investigation and indicates a multidimensional chaotic dynamics and, generally speaking, multimode excitations in the resonance system in question. The extent of its stochastization is quite high, which follows from the estimate of correlation dimension in the range of small r . It should be noted that recent investigations of parametric resonance in a related metallorganic antiferromagnet³¹ also confirms the deterministic origin of noise in these compounds.

The existing theories of relaxation oscillations^{3,8,9,29,32} make it possible to describe the emergence of high-dimensional chaos on the basis of multimode models. The main idea behind the mechanism of emergence of relaxation oscillations can be demonstrated even by using a two-mode model in which it is assumed that the resonance excitation conditions are satisfied for one mode and are not observed for the other mode. Under the action of pumping, such a pair of coupled nonlinear oscillators reproduces quantitatively the behavior of relaxation oscillations. A quantitative theory of this effect for antiferromagnets has not been developed as yet. However, a theoretical description of this phenomenon in the approximation of two spins simulating the sublattices subjected to resonant transverse and

longitudinal pumping appears as promising. Consequently, chaotic relaxation oscillations can be described qualitatively as the dynamics of a nonlinear oscillator under resonance conditions, but under the action of certain random forces (the inclusion of the effect of the second oscillator). Such a system may have at least two stable states the transition between which can lead to the emergence of spike-like and saw-tooth time dependences of absorbed power. The features and diversity of existing chaotic modes are obviously determined by the time of residence of the system in the equilibrium states and the rate of transient processes. Such a system can obviously have a high degree of stochastization, an attempt to create regular attractors in it will lead to regimes in which such attractors coexist with a well-developed dynamic noise. However, a quantitative theory of such chaotic oscillations should apparently be constructed on the basis of a multimode model according to the numerical analysis carried out by Moser et al.³²

The theorem on dimension that has been formulated recently for systems with a dynamic noise indicates in its simplified formulation the additivity of the dimension of a regular attractor and a noise.⁴⁰ In this sense, these can be separated, and the question of elimination of noise from a signal, at least the noise reduction, and isolation of a regular signal from the data on temporal series appears as justified.

There are effective methods of suppression of noise effect on the useful signal.³⁸ These methods are extremely effective for reduction of external additive noise, but their application in the case of a dynamic noise should be verified in each specific case. The algorithm of purification of a signal in the simplest form can be described as follows. In the chosen embedding space whose dimension is larger than the sum of the predicted dimension of the regular attractor and dynamic noise, the nearest neighbors of the preferred vector of state are selected, and its central coordinate is averaged over the values of relevant coordinates of the found neighbors. The obtained sequence of new data is the result of one iteration that can be repeated. Such an algorithm can be optimized as well as the choice of required parameters (correlation radius, dimension, etc.; see Ref. 38). Such an algorithm will be used below for analyzing the chaotic temporal series measured by us.

On the other hand, the above algorithm in the simplest form includes the conventional method of data averaging over nearest and next to nearest neighbors in the series. In this case, the dimension of the embedding space is equal to unity, and the number of neighbors is fixed. It can easily be verified that in spite of its very simple form, the procedure operates as a high-frequency filter and does not change the complex low-frequency spectrum of chaotic oscillations. We shall apply this procedure also to analyze the results.

We chose the object of investigation in the form of a chaotic attractor obtained from the temporal series presented in Fig. 2*b*. The results of analysis are shown in Fig. 10 (it should be noted that the average value is subtracted from the terms of the series). Figures 10*a* and *b* show the phase portrait on the plane $\{V(t), V(t+\tau)\}$, where $\tau = 29.5$ ms, and simultaneously the map for the data on the Poincarè cross section (see above), while Figs. 10*c, d, e,* and *f* contain the dependences for the data “corrected” by the method of averaging and the optimized method of noise reduction described above respectively (averaging was carried out twice over five points, and tenfold iterations were used in the optimized method).

Figures 10*e* and *f* clarify the internal structure of a regular attractor. After the effect of noise becomes weaker, its phase portrait resembles a strange multiband attractor. The analysis of correlation dimension makes it possible to characterize quantitatively both the regular attractor as well as the residual contribution of deterministic noise. The results of analysis are presented in Fig. 11. It should be noted that prior to calculation correlation functions for the temporal series under consideration, we initially normalized all values to a unit interval by the formula $\tilde{V}(t_i) = (V(t_i) - V_{\min}) / (V_{\max} - V_{\min})$, where V_{\min} and V_{\max} are the minimum and maximum values of the signal in the series. It was found that the dimensionality of a regular attractor can be estimated as 2.15 ± 0.05 , and the total dimensionality with the contribution of deterministic noise as 3.25 ± 0.05 . Spectral analysis of these “improved” results also indicate that the quantitative contribution of noise remained quite large, and the resultant attractor possesses a high dimensionality as before.

Thus, chaotic dynamics in the nonlinear antiferromagnetic resonance in low-dimensional antiferromagnets is high-dimensional, the extent of stochastization of oscillations is high,

and noise has a deterministic origin and serves as a decisive factor in nonlinear dynamics of these magnets.

Finally, we formulate the following conclusions following from our analysis.

1. Peculiarities of a transition to chaos by “irregular periods” in a $2D$ metallorganic antiferromagnet with an “easy axis” type anisotropy are experimentally observed and studied in detail under conditions of nonlinear antiferromagnetic resonance.
2. It is shown that relaxation oscillations of absorbed power are generated for very low energy levels of microwave field and have a low frequency of fundamental harmonic (of the order of a few hertz). No multiple harmonics are observed experimentally at kilohertz and higher frequencies.
3. Relaxation oscillations at low values of driving power exist in the form of generally periodic sequence of spike-like peaks of absorbed power. The frequency spectrum contains components of fundamental frequency corresponding to the emergence of spikes as well as multiple harmonics, which demonstrates a nonlinear nature of the process.
4. As the pumping amplitude increases, the phenomenon of period doubling is observed in the time dependence of absorbed energy of microwave field. The shape of the signal is simultaneously transformed from the spike-like to the saw-tooth type having segments with linearly increasing and linearly decreasing absorption. An analysis of the frequency–amplitude dependence of oscillations and their linear autocorrelation function gives quantitative characteristics of this transition.
5. A similar effect is observed at a fixed level of pumping, but upon a change in the value of static magnetic field near its resonant value.
6. With increasing power, relaxation oscillations become chaotic. The spectrum of such oscillations is continuous and has a “grass-like” form, but the peaks of fundamental

harmonics are still distinguishable. The phase portrait of these oscillations has the form of a strange attractor experiencing a strong influence of noise. Stochastization of oscillations, however, is not a result of influence of an additive instrumental noise.

7. The quantitative characteristics of such a strange attractor are calculated. The one-dimensional map corresponding to the given attractor demonstrates a tendency to regular movement in spite of chaotic time dependence of relaxation oscillations. An analysis of correlation dimension indicates the high-dimensional chaos dynamics and the deterministic nature of noise in the magnetic system under investigation. The possibility of formal separation of the regular movement and the noise contribution with the help of nonlinear methods of noise reduction being developed is considered.
8. The applicability of the theoretical model of finite number of coupled spins under the action of the parametric and transverse pumping to the construction of a quantitative theory of the scenario of transition to chaos by “irregular periods” is discussed briefly. The transition can be regarded as a universal phenomenon in low-dimensional ferro- and antiferromagnets under nonlinear resonance conditions.

ACKNOWLEDGEMENTS

The authors are grateful to S. V. Volotskii for fruitful discussions and to H. Kantz, R. Hegger, and Th. Schreiber for valuable advice and help in carrying out a number of calculations.

REFERENCES

- ¹ G. Gibson and C. Jeffries, *Phys. Rev.* **A29**, 811 (1984).
- ² H. Yamazaki, *J. Phys. Soc. Jpn.* **53**, 1155 (1984).
- ³ F. Waldner, R. Badii, D. R. Barberis, et al., *J. Mag. Mag. Mater.* **54–57**, 1135 (1986).
- ⁴ H. Yamazaki and M. Warden, *J. Phys. Soc. Jpn.* **55**, 4477 (1986).
- ⁵ F. M. de Aguiar and S. M. Rezende, *Phys. Rev. Lett.* **56**, 1070 (1986).
- ⁶ A. I. Smirnov, *Zh. Eksp. Teor. Fiz.* **90**, 385 (1986) [*Sov. Phys.–JETP* **63**, 222 (1986)].
- ⁷ H. Yamazaki, M. Mino, H. Nagashima, and M. Warden, *J. Phys. Soc. Jpn.* **56**, 742 (1987).
- ⁸ P. Bryant, C. Jeffries, and K. Nakamura, *Phys. Rev.* **A38**, 4223 (1988).
- ⁹ M. Warden and F. Waldner, *J. Appl. Phys.* **64**, 5386 (1988).
- ¹⁰ A. I. Smirnov, *Zh. Eksp. Teor. Fiz.* **94**, 185 (1988) [*Sov. Phys.–JETP* **67**, 969 (1988)].
- ¹¹ T. L. Carrol, L. M. Pecora, and F. J. Rachford, *J. Appl. Phys.* **64**, 5396 (1988).
- ¹² H. Benner, F. Rodelsperger, H. Seitz, and G. Wiese, *J. Phys.* **C8**, 1603 (1988).
- ¹³ P. E. Wigen, H. Doetsch, Y. Ming, et al., *J. Appl. Phys.* **63**, 4157 (1988).
- ¹⁴ A. A. Stepanov, M. I. Kobets, and A. I. Zvyagin, *Fiz. Nizk. Temp.* **9**, 764 (1983) [*Sov. J. Low Temp. Phys.* **9**, 391 (1983)].
- ¹⁵ A. I. Zvyagin, M. I. Kobets, V. N. Krivoruchko, et al., *Zh. Eksp. Teor. Fiz.* **89**, 2298 (1985) [*Sov. Phys.–JETP* **62**, 1328 (1985)].
- ¹⁶ A. A. Stepanov, V. A. Pashchenko, and M. I. Kobets, *Fiz. Nizk. Temp.* **14**, 550 (1988) [*Sov. J. Low Temp. Phys.* **14**, 304 (1988)].
- ¹⁷ A. A. Stepanov, V. A. Pashchenko, and M. I. Kobets, *Fiz. Nizk. Temp.* **14**, 1212 (1988) [*Sov. J. Low Temp. Phys.* **14**, 669 (1988)].

- ¹⁸ A. A. Stepanov, A. I. Zvyagin, S. V. Volotskii, et al., *Fiz. Nizk. Temp.* **15**, 100 (1989) [*Sov. J. Low Temp. Phys.* **15**, 57 (1989)].
- ¹⁹ H. Yamazaki and M. Mino, *Progr. Theor. Phys. Suppl. No. 98*, 400 (1989).
- ²⁰ J.-P. Eckmann, *Rev. Mod. Phys.* **53**, 643 (1981).
- ²¹ M. Feigenbaum, *Usp. Fiz. Nauk* **141**, 343 (1983) [*Sov. Phys.–Uspekhi* **26**, (1983)].
- ²² J.-P. Eckmann and D. Ruelle, *Rev. Mod. Phys.* **57**, 617 (1985).
- ²³ V. E. Zakharov, V. S. L’vov, and S. S. Starobinets, *Usp. Fiz. Nauk* **114**, 609 (1974) [*Sov. Phys.–Uspekhi* **17**, 896 (1975)].
- ²⁴ V. V. Zautkin, V. S. L’vov, and S. S. Starobinets, *Zh. Eksp. Teor. Fiz.* **63**, 182 (1973) [*Sov. Phys.–JETP* **36**, 96 (1973)].
- ²⁵ V. V. Zautkin, V. S. L’vov, and S. S. Starobinets, *Fiz. Tverd. Tela (Leningrad)* **16**, 678 (1974) [*Sov. Phys.–Solid State* **16**, 446 (1974)].
- ²⁶ H. Benner, F. Roedelsperger, and G. Wiese, in: *Nonlinear Dynamics in Solids* (ed. by H. Thomas), Springer, Berlin, Heidelberg (1992).
- ²⁷ F. M. de Aguiar, A. Azevedo, and S. M. Rezende, *Phys. Rev.* **B39**, 9448 (1989).
- ²⁸ T. S. Hartwick, E. R. Peressini, and M. T. Weiss, *J. Appl. Phys., Suppl.* **32**, 223S (1961).
- ²⁹ F. Waldner, D. R. Barberis, and H. Yamazaki, *Phys. Rev.* **A31**, 420 (1985).
- ³⁰ F. Waldner, *J. Phys.* **C21**, 1243 (1988).
- ³¹ M. Warden, *Phys. Rev.* **E48**, R639 (1993).
- ³² H. R. Moser, P. F. Meier, and F. Waldner, *Phys. Rev.* **B47**, 217 (1993).
- ³³ H. Arend, K. Tichy, K. Baberschke, and F. Rys, *Solid State Commun.* **18**, 999 (1976).
- ³⁴ K. Tichy, J. Benes, R. Kind, and H. Arend, *Acta Cryst.* **B36**, 1355 (1980).

- ³⁵ M. T. Weiss, Phys. Rev. Lett. **1**, 239 (1958).
- ³⁶ N. Gershenfeld, in: *Directions in Chaos*, vol. 2 (ed. by Hao Bai-lin), World Scientific, Singapore (1988).
- ³⁷ H. D. I. Abarbanel, R. Brown, J. J. Sidorowich, and L. Sh. Tsimring, Rev. Mod. Phys. **65**, 1331 (1993).
- ³⁸ H. Kantz and Th. Schreiber, *Nonlinear Time Series Analysis*, Cambridge Univ. Press, Cambridge (UK) (1997).
- ³⁹ I. S. Aranson, A. M. Reiman, and V. G. Shekhov, in: *Nonlinear Waves. Dynamics and Evolution* (ed. by A. V. Gaponov-Grekhov and M. I. Rabinovich), [in Russian], Nauka, Moscow (1989).
- ⁴⁰ M. R. Muldoon, D. S. Broomhead, J. P. Huke, and R. Hegger, Dynamics and Stability of Systems **13**, 175 (1998).

FIGURES

FIG. 1. Amplitude–field dependences of nonlinear antiferromagnetic resonance for a 2C4Mn crystal for different values of driving power. The bold segment on the upper curve in the vicinity of the high-field peak denotes the range of relaxation oscillations. The hysteresis loop observed for a power exceeding -5 dB increases with driving power.

FIG. 2. Chaotic oscillations of absorbed power and their frequency spectrum for a driving power of 5 mW for a resonant curve with closely spaced peaks in fields $H_m = 8.37$ kOe (*a*) and 8.4 kOe (*b*).

FIG. 3. Evolution of time dependences of absorbed power for a change in the microwave power level from -10 to 0 dB for a static magnetic field $H = 8.4$ kOe.

FIG. 4. Frequency of relaxation oscillations as a function of driving power. Solid and open circles correspond to an increase and decrease in the driving power respectively. The threshold effect of oscillation period doubling is of the hysteresis type.

FIG. 5. Temporal series of absorbed power and their spectra for different values of static magnetic field for the driving power $P = -1$ dB : (*a*) $H = 8.51$ kOe, relaxation oscillations with a spike-like structure and a high stochastization level; (*b*) $H = 8.47$ kOe, the result of transformation of spike-like signals into saw-tooth signals; (*c*) $H = 8.44$ kOe, saw-tooth relaxation oscillations with linearly increasing and decreasing segments; (*d*) $H = 8.39$ kOe, chaotic temporal series with an intense “grass-like” frequency spectrum; (*e*) $H = 8.34$ kOe (*e*), nearly regular anharmonic oscillations of absorbed power of a spike-like shape. All the spectra contain the peak of the fundamental frequency of relaxation oscillations of the order of several hertz and its higher harmonics as well as the peak of the reference frequency 50 Hz and combination frequencies.

FIG. 6. Dependence of “time delay” τ on the pumping power P . The value of τ is measured in units of the temporal series period $\Delta t = 4.9$ ms.

FIG. 7. Dynamic characteristics of relaxation oscillations for the driving power $P = 0$ dB and $H = 8.4$ kOe, whose time dependence is shown in Fig. 3: (a) phase portrait in the time-delay coordinates ($\tau = 49$ ms) and (b) one-dimensional map constructed from the sequence of minimum values of the Poincarè cross section of the phase portrait taken at the instants of time t_m at which $V(t_m) = 0$.

FIG. 8. Amplitude peaks and interspike intervals for relaxation oscillations for driving power $P = 0$ dB and $H = 8.4$ kOe (see Fig. 3) (a, c), and $P = 1$ dB and $H = 8.51$ kOe (see Fig. 5a) (b, d).

FIG. 9. Dependences of logarithms of correlation integrals on the logarithm of the distance between vectors in the m -dimensional embedding space calculated from the initial integral data for the attractor presented in Fig. 7.

FIG. 10. Phase portraits and one-dimensional map for relaxation oscillations for the driving power 5 mW in the field $H = 8.4$ kOe in the case of closely spaced peaks on the resonant curves (see Fig. 2b) for original data on temporal series (after the subtraction of the average value) (a, b), for doubly averaged data for five nearest neighbors (c, d), and for data “improved” by the optimized method of noise suppression as a result of ten iterations (e, f).

FIG. 11. Dependences of logarithms of correlation integrals on the logarithm of the distance between vectors in the m -dimensional embedding space calculated for data “improved” by the optimized method (see Figs. 10e, f).

This figure "fig1.gif" is available in "gif" format from:

<http://arxiv.org/ps/nlin/0104032v1>

This figure "fig2.gif" is available in "gif" format from:

<http://arxiv.org/ps/nlin/0104032v1>

This figure "fig3.gif" is available in "gif" format from:

<http://arxiv.org/ps/nlin/0104032v1>

This figure "fig4.gif" is available in "gif" format from:

<http://arxiv.org/ps/nlin/0104032v1>

This figure "fig5.gif" is available in "gif" format from:

<http://arxiv.org/ps/nlin/0104032v1>

This figure "fig6.gif" is available in "gif" format from:

<http://arxiv.org/ps/nlin/0104032v1>

This figure "fig7a.gif" is available in "gif" format from:

<http://arxiv.org/ps/nlin/0104032v1>

This figure "fig7b.gif" is available in "gif" format from:

<http://arxiv.org/ps/nlin/0104032v1>

This figure "fig8.gif" is available in "gif" format from:

<http://arxiv.org/ps/nlin/0104032v1>

This figure "fig9.gif" is available in "gif" format from:

<http://arxiv.org/ps/nlin/0104032v1>

This figure "fig10.gif" is available in "gif" format from:

<http://arxiv.org/ps/nlin/0104032v1>

This figure "fig11.gif" is available in "gif" format from:

<http://arxiv.org/ps/nlin/0104032v1>